OFFICE OF NAVAL RESEARCH

Contract N00014-76-C-0200

Task No. NR 356-504

TECHNICAL REPORT NO. 26

EFFECT OF THE EXTENT OF CURE ON THE MODULUS, GLASS TRANSITION, WATER ABSORPTION, AND DENSITY OF AN AMINE-CURED EPOXY

by

John B. Enns and John K. Gillham

for publication in

Journal of Applied Polymer Science

PRINCETON UNIVERSITY
Polymer Materials Program
Department of Chemical Engineering
Princeton, New Jersey 08544

April 1983

Principal Investigator
John K. Gillham
(609) 452-4694

SECURITY CLASSIFICATION OF THIS PAGE (When Data Entered)

REPORT DOCUMENTATION PAGE

READ INSTRUCTIONS BEFORE COMPLETING FORM

1. REPORT NUMBER: Technical Report #26	2. GOVT ACCESSION NO.: AD-A127090
3. RECIPIENT'S CATALOG NUMBER	
4. TITLE (and Subtitle): Effect of the Extent of Cure on the Modulus, Glass Transition, Water Absorption, and Density of an Amine-Cured Epoxy	5. TYPE OF REPORT & PERIOD COVERED: April 1981-April 1983
	6. PERFORMING ORG. REPORT NUMBER
7. AUTHOR(s): John B. Enns and John K. Gillham	8. CONTRACT OR GRANT NUMBER(s): N00014-76-C-0200
9. PERFORMING ORGANIZATION NAME AND ADDRESS: Polymer Materials Program, Department of Chemical Engineering, Princeton University, Princeton, NJ 08544	10. PROGRAM ELEMENT, PROJECT, TASK AREA & WORK UNIT NUMBERS: Task No. NR 356-504
11. CONTROLLING OFFICE NAME AND ADDRESS: Office of Naval Research, 800 North Quincy St., Arlington, VA 22217	12. REPORT DATE: April 1983
	13. NUMBER OF PAGES: 40
14. MONITORING AGENCY NAME & ADDRESS(if different from Controlling Office)	15. SECURITY CLASS. (of this report)
	15a. DECLASSIFICATION/DOWNGRADING SCHEDULE

16. DISTRIBUTION STATEMENT (of this Report)

Approved for Public Release; Distribution Unlimited.

17. DISTRIBUTION STATEMENT (of the abstract entered in Block 20, if different from Report)

18. SUPPLEMENTARY NOTES

APR 22 1983

A

19. KEY WORDS (Continue on reverse side if necessary and identify by block number)

Torsion Pendulum
Torsional Braid Analysis
Transitions
Density of Epoxy
Modulus of Epoxy
Water Absorption of Epoxy
Free Volume of Epoxy
Epoxy Cure
Time-Temperature-Transformation Cure Diagrams

20. ABSTRACT (Continue on reverse side if necessary and identify by block number)

The modulus, density, glass transition (Tg), and water absorption characteristics of an amine-cured resin [diglycidyl ether of bisphenol A (Epon 828)/diaminodiphenyl sulfone (DDS)] were studied as a function of extent of cure. The glass transition is a function of the extent of cure and reaches a maximum temperature, $T_{g\infty}$, when it is completely cured; specimens with different extents of cure were formed by isothermal cure below $T_{g\infty}$ for different times. After slowly cooling, the density at each extent of cure was obtained at room

DD FORM 1 JAN 73 1473 EDITION OF 1 NOV 65 IS OBSOLETE
S/N 0102-LF-014-6601

SECURITY CLASSIFICATION OF THIS PAGE (When Data Entered)

temperature. Moisture absorption was monitored gravimetrically at 25°C for two months at several humidity levels. The room temperature density and modulus decreased with increasing extent of conversion whereas the glass transition temperature and equilibrium water absorption increased. The equilibrium water absorption increased linearly with relative humidity, and the absorptivity increased linearly with specific volume. An interpretation of these anomalous results is made in terms of the nonequilibrium nature of the glassy state. The glass transition temperature increases as the extent of cure increases resulting in a material that is further from equilibrium at room temperature and therefore having more free volume and a greater propensity to absorb water.

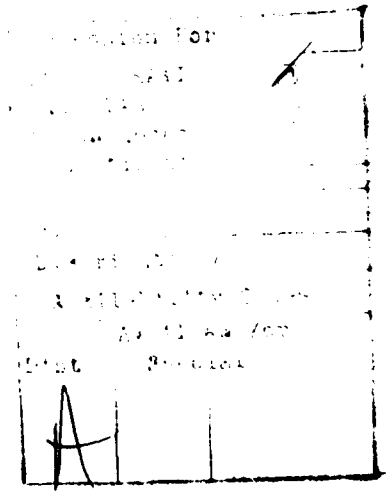

EFFECT OF THE EXTENT OF CURE ON THE MODULUS, GLASS TRANSITION, WATER ABSORPTION, AND DENSITY OF AN AMINE-CURED EPOXY

John B. Enns* and John K. Gillham
Polymer Materials Program
Department of Chemical Engineering
Princeton University
Princeton, New Jersey 08544

Synopsis

The modulus, density, glass transition (Tg), and water absorption characteristics of an amine-cured resin [diglycidyl ether of bisphenol A (Epon 828)/diaminodiphenyl sulfone (DDS)] were studied as a function of extent of cure. The glass transition is a function of the extent of cure and reaches a maximum temperature, Tg_∞, when it is completely cured; specimens with different extents of cure were formed by isothermal cure below Tg_∞ for different times. After slowly cooling, the density at each extent of cure was obtained at room temperature. Moisture absorption was monitored gravimetrically at 25°C for two months at several humidity levels. The room temperature density and modulus decreased with increasing extent of conversion whereas the glass transition temperature and equilibrium water absorption increased. The equilibrium water absorption increased linearly with relative humidity, and the absorptivity increased linearly with specific volume. An interpretation of these anomalous results is made in terms of the nonequilibrium nature of the glassy state. The glass transition temperature increases as the extent of cure increases resulting in a material that is further from equilibrium at room temperature and therefore having more free volume and a greater propensity to absorb water.

*Present address: Bell Laboratories, Whippany, NJ 07981.

INTRODUCTION

The curing phenomena of a thermosetting epoxy resin can be understood in terms of a time-temperature-transformation (TTT) cure diagram (1) in which the times to gelation and vitrification are plotted versus the isothermal cure temperature. As can be seen in Figure 1, the "S"-shaped vitrification curve and the gelation curve divide the time-temperature plot into four distinct states of matter: liquid, gelled rubber, ungelled glass, and gelled glass. Tg_o is the glass transition temperature of the unreacted resin mixture, Tg_∞ is the glass transition of the fully cured resin, and $_{gel}Tg$ is the glass transition of the resin at its gel point.

The times to gelation and vitrification can be determined from the loss peaks of an isothermal dynamic mechanical spectrum obtained using the torsional braid analysis (TBA) technique (2). At cure temperatures sufficiently below Tg_∞ the reaction will not go to completion because, as the viscosity increases (a result of the increasing molecular weight), the reaction becomes diffusion controlled and eventually is quenched as the material vitrifies (3). The extent of conversion attained when the reaction is quenched increases as the cure temperature is raised, as evidenced by a corresponding increase in the glass transition temperature.

In addition to the increase in glass transition temperature, other parameters can be monitored as a function of the extent of cure in an attempt to understand the changes that occur during cure. These include the shear modulus (of a film which can be measured with a torsion pendulum), the room temperature density, and the room temperature equilibrium water absorption.

In this paper, the above mentioned techniques, as well as gel fraction experiments to identify the gel time in the dynamic mechanical spectra (4), have been used to monitor the changes in physical properties that occur during cure. A preliminary report from this laboratory has been published (5).

EXPERIMENTAL

Materials

A stoichiometric mixture of the diglycidyl ether of bisphenol A (Epon 828: Shell) and 4,4'-diaminodiphenyl sulfone (DDS: Aldrich) was prepared for the investigation (see Figure 2). For the TBA experiments each of the components was dissolved in methylethylketone (MEK) before mixing. For the other experiments the amine was added after the epoxy had been heated to 130°C; the mixture was stirred until the amine dissolved in the epoxy (< 5 min). Equal amounts (by weight) of the neat resin were poured into aluminum foil-lined aluminum molds (2" × 1/2" × 1/16"), degassed in a vacuum oven (∿ 1 Torr) at 80°C for 20 min (until the bubbles disappeared), and placed in a heated oven (purged with nitrogen) at 175°C to cure. After curing for specified times (50, 100, 180, and 600 min) the specimens were allowed to cool slowly to room temperature in the oven and then were placed in a dessicator. The cured specimens were clear, indicating that the mixture had not phase-separated during the process.

Torsional Braid Analysis (TBA)

Supported TBA specimens were made by dipping a multifilamented glass braid into a resin/MEK solution (20% resin). They were then mounted in the specimen chamber in a helium atmosphere at the temperature of cure, and their modulus and logarithmic decrement were monitored by an automated apparatus (2)

until the reaction was either complete or quenched, as indicated by a leveling off of the modulus. Typically, two peaks in logarithmic decrement were observed during cure, identified as a liquid-to-rubber transformation (gelation) and a rubber-to-glass transformation (vitrification), respectively. Representative spectra are shown in Figure 3, and the times to these events are tabulated in Table I. Thermomechanical spectra were then obtained on cooling to -190°C (at 1.5°C/min) and heating to 250°C (at the same rate). By heating the partially cured resin to 250°C (i.e., above Tg_∞ = 210°C) it can be cured fully. A subsequent scan from 250 to -190°C provides the spectrum of the fully cured resin. However, the variation of Tg_∞ with thermal prehistory indicates that thermal degradation had occurred on heating to 250°. Two major relaxations are observed in these spectra: the glass transition (Tg) and a secondary subglass transition (T_{sec}) related to the motion of the $-CH_2-CH(OH)-CH_2-O-$ group in the epoxy (6). The values of T_{sec}, $T_{sec\infty}$, Tg and Tg_∞ obtained from these scans are tabulated in Table I and plotted in Figure 4. T_{sec} and Tg increase with increasing extent of cure to approach $T_{sec\infty}$ and Tg_∞, respectively. It is noted that the glass transition temperature after prolonged isothermal cure is higher than the temperature of cure (4, 7).

In order to monitor the increase in the glass transition during isothermal cure at 175°C, the cure was interrupted at selected times (using separate samples), and a temperature scan made to determine the glass transition temperature. The spectra of the partially cured specimens and subsequently fully cured specimens are shown in Figure 5; the glass transition temperatures versus time of cure are shown in Figure 6. Note that the cure time was insufficient to fully cure the resin.

Torsion Pendulum

A film of Epon 828/DDS, prepared as described above by partially curing at 175°C for 100 min., was machined to dimensions of 4.70 × 0.60 × 0.063 cm and mounted in a calibrated torsion pendulum (2). Thermomechanical spectra displaying quantitative values of the elastic shear modulus (G') and logarithmic decrement (Δ) of the partially cured specimen were obtained on cooling to -190°C (not shown in Figure 7) and subsequent heating (Figure 7) to 250°C. The spectrum of the fully cured film was then obtained on cooling to -190°C (Figure 7).

Gel Fraction

Two independent experiments were conducted to estimate the gel times of the resin at various temperatures; in one the reaction was conducted in an air atmosphere, whereas in the other a helium atmosphere was used. In the former case, open test tubes containing approximately 5 ml of resin were placed in a heated oil bath held at a series of fixed temperatures. The test tubes wre removed at selected intervals, cooled, and the soluble portion extracted with MEK for 48 hours. The insoluble portion (gel) was then dried, weighed and compared with the initial weight (before extraction) to give a gel fraction. This procedure was carried out with 11 or more samples at each of 10 cure temperatures ranging from 102 to 202°C; the data are shown in Figures 8a and 8b.

In the second experiment, 1 to 2 ml of resin were placed in ampules, degassed for 20 minutes (until the bubbles disappeared) at 1 torr, sealed in a helium atmosphere, and placed in a heated oil bath held at a fixed temperature. The ampules were removed at selected intervals, quenched in

liquid nitrogen, broken, and the soluble portion extracted with MEK for 3 hours using a Soxhlet extraction column with coarse thimbles. The insoluble portion (gel) was then dried, weighed and compared with the initial weight (before extraction) to give a gel fraction. This procedure was carried out at each of seven cure temperatures ranging from 132 to 184°C; the data are shown in Figure 8c. The gel points for both experiments, defined as the onset of insolubility, and calculated using the zero intercept of the extrapolated gel fraction curves, are tabulated in Table II.

Water Absorption

Films of Epon 828/DDS were prepared as described above for different times of cure at 175°C; i.e. 50, 100, 180, and 600 minutes. The specimens were prepared in order of diminishing cure time; the 600 min. cured specimens were prepared first, and the 50 min. cured specimens were cured last, so that changes due to aging would minimize rather than enhance differences in density between the specimens (5). After the specimens had been stored in a vacuum oven at 50°C for 2 days, three specimens of each degree of cure were exposed to each of 4 different relative humidity atmospheres, 31, 51, 79.3 and 93%, generated by saturated solutions of calcium chloride hexahydrate, calcium nitrate, ammonium chloride and ammonium dihydrogen phosphate, respectively, at 25 ± 0.5°C. Each film was suspended by a hook over a saturated salt solution in a sealed test tube. The moisture uptake was measured by intermittently removing the films from the test tubes and weighing them on a microbalance. The average percent weight gain of three specimens is plotted vs. $(\text{time})^{\frac{1}{2}}$ in Figures 9 to 12 for each of the relative humidities to which they were

exposed. [A more rigorous approach would have involved plotting percent weight gain vs. $(\text{time})^{\frac{1}{2}}$/thickness.]

After 2000 hours of exposure the samples were dried in a vacuum oven at 50°C for two weeks; their weight came to within 0.028% ± 0.060 of the initial weight.

Density

Densities of the cured epoxy specimens were measured in a density gradient column (ASTM D1505) at 25°C, prepared from mixtures of o-dichlorobenzene and toluene, which had been calibrated with calibration floats with densities 1.2320, 1.2344 and 1.2379 g/ml. Densities of specimens were determined by interpolating the calibration curve at the levels at which they came to rest (Figure 13). Measurements were made one hour after lowering the specimens into the column since their positions drifted over the course of several days due to swelling.

RESULTS AND DISCUSSION

A TTT diagram for Epon 828/DDS was constructed (Figure 14) using the information obtained from the TBA and gel fraction experiments. A comparison of the gel fraction data with the TBA liquid-to-rubber transformation in a ℓn (time) versus 1/T plot (Figure 15) indicates that there is a direct correlation between gelation and the liquid-to-rubber transformation. This relationship was also observed in the Epon 825/DDS and Epon 834/DDS systems (3,8), whereas the correlation is not as good for the Epon 828/PACM-20 system (3). Only the top portion (above 80°C) of the TTT diagram for Epon 828/DDS (Figure 14) was obtained, since the presence of the solvent might have affected the TBA

spectrum (bp MEK = 79°C). Using the TTT diagram and the Tg versus T_{cure} plot (Figure 4), a cure temperature could be chosen (175°C) at which the glass transition of the cured resin should eventually approach Tg_{∞} (Figure 6). A reason for using one temperature to study the effect of the extent of cure on the physical properties is to eliminate the effect of other factors. For example, the reaction mechanism might be temperature dependent, or the fractional free volume locked into the crosslinked network may be a function of the cure temperature (9).

Although the equilibrium modulus might be expected to increase with increasing crosslink density, the modulus between T_{sec} and Tg (Figure 7) of the fully-cured film is lower than that of the partially cured film. This apparently anomalous result will be discussed later in the light of the other results.

The absorption of water by an epoxy film has been considered to occur by simple Fickian diffusion. The moisture concentration in a thin film at constant temperature can be described by Fick's second law for one-dimensional diffusion:

$$\frac{\partial c}{\partial t} = D_x \frac{\partial^2 c}{\partial x^2} \qquad (1)$$

where c is the moisture concentration at time t, D_x is the diffusivity of the material in the direction normal to the surface, and x is the distance into the film from the surface. On solving equation 1 and integrating over the film thickness (10), the percent moisture content M (% weight gain) of the material as a function of time is

$$M = G(M_{\infty} - M_o) + M_o \qquad (2)$$

where M_o is the initial moisture content, M_∞ is the equilibrium moisture content, and G is a time dependent parameter

$$G = 1 - \frac{8}{\pi^2} \sum_{i=0}^{\infty} \exp \frac{[-(2i+1)^2\pi^2 \, D_x t/h^2]}{(2i+1)^2} \tag{3}$$

which can be approximated (11) by

$$G = 1 - \exp[-7.3 \, (D_x t/h^2)^{0.75}] \tag{4}$$

where h is the film thickness.

The diffusivity D is obtained from the initial slope of the M versus $\sqrt{t}$ curve

$$D = \pi \left(\frac{h}{4M_\infty}\right)^2 \left(\frac{M_2 - M_1}{\sqrt{t_2} - \sqrt{t_1}}\right)^2 \tag{5}$$

and, if the moisture entering the specimen through the edges is considered,

$$D_x = \frac{D}{(1 + \frac{h}{\ell} + \frac{h}{w})^2} \tag{6}$$

where ℓ is the length and w is the width of the specimen (11).

The equilibrium moisture content is a function of the relative humidity, ϕ, of the air to which it is exposed (12):

$$M_\infty = a\phi^b \tag{7}$$

The constants a (absorptivity) and b are selected to provide the best fit to the data.

The equilibrium moisture level M_∞ and diffusivity D_x of the films at each of the extents of cure and relative humidity can be obtained directly from Figures 9 to 12 and are tabulated in Table III. Although there was considerable scatter in the equilibrium moisture content of specimens that had the same cure history and relative humidity exposure, the trends were the same for each of the levels of relative humidity, with one exception [the film cured for 180 minutes had a higher equilibrium moisture content than the film cured for 600 minutes after exposure to 31% relative humidity (Figure 9)]. In general, the films that were cured to a greater extent showed a higher equilibrium moisture content.

The diffusivity data show even greater scatter, and thereby perhaps provide a clue to some of the problems inherent in the experiment. Although the diffusivity is expected to remain constant with respect to relative humidity, it varies as much with relative humidity as it does with extent of cure. Unusually high values were observed for 51% relative humidity, which is an indication that something unanticipated occurred with that set of specimens.

The equilibrium moisture content of the films cured to different extents is plotted versus relative humidity in Figure 16. Since b (in equation 7) is equal to one, the slopes provide the absorptivities (a) which are seen to increase with increasing extent of cure. Both the higher equilibrium moisture content and higher absorptivity with increasing cure suggest increasing free volume, and hence an increasing specific volume with increasing cure. This is borne out by the density measurements, which indicate that the room temperature density decreases with increasing cure. Although this is in agreement with the work of Shimazaki (13), it runs contrary to conventional wisdom (14, 15). A linear plot of absorptivity vs. specific volume (Figure 17) suggests that a linear relationship exists between absorptivity and free volume:

$$a = KV$$

where K = 4.05 g/ml.

The key to understanding this apparently anomalous behavior is to note that the temperature at which the density and water absorption were measured (25°C) was below the glass transition temperature. Schematic plots of specific volume versus temperature for a partially cured and fully cured material are shown in Figure 18. In the rubbery state above the glass transition temperature, the density of the more highly crosslinked material is higher; but its Tg is also higher, and as a result the specific volume versus temperature curves can cross (13), resulting in a lower density at room temperature for the more highly crosslinked material. The lower room temperature modulus (6, 16) for a more highly crosslinked material can now be understood as well, since it is directly proportional to density.

This dependence of specific volume at room temperature on the glass transition has also been observed in amorphous linear polymers. Ueberreiter and Kanig (17) demonstrated that the room temperature density of polystyrene decreased as its molecular weight (and Tg) increased.

CONCLUSIONS

These experiments on epoxy resin have shown that the lower modulus and higher equilibrium moisture content of the more highly cured resins at room temperature are a consequence of the lower density which in turn is a result of the increase in Tg as a function of cure. At room temperature the more highly cured material is further from equilibrium, and therefore has more free volume than a material cured to a lesser extent.

Acknowledgment. Partial financial support was provided by the Chemistry Branch of the office of Naval Research.

REFERENCES

1. J. K. Gillham, Torsional Braid Analysis (TBA) of Polymers. In Developments in Polymer Characterization-3. Ed., J. V. Dawkins. Applied Science Publishers, Ltd., London, pp. 159-227 (1982).

2. J. B. Enns and J. K. Gillham, Automated Torsion Pendulum: Control and Data Collection/Reduction Using a Desktop Computer. In Computer Applications in Applied Polymer Science. Ed., T Provder. American Chemical Society Symposium Series, No. 197, pp. 329-352 (1982).

3. J. B. Enns and J. K. Gillham, J. Appl. Polym. Sci. In press (1983).

4. J. B. Enns and J. K. Gillham, Torsional Braid Analysis: Time-Temperature-Transformation Cure Diagrams of Thermosetting Epoxy/Amine Systems. In Polymer Characterization: Spectroscopic, Chromatographic, and Physical Instrumental Methods. Ed., C. D. Craver, Advances in Chemistry Series, No. 203, American Chemical Society, Washington, D.C. 1983.

5. J. P. Aherne, J. B. Enns, M. J. Doyle and J. K. Gillham, Division of Organic Coatings and Plastics Chemistry, Preprints, 46, 574 (1982).

6. G. A. Pogany, Polymer 11, 66 (1970).

7. N. S. Schneider and J. K. Gillham, Polymer Composites, 1, 97 (1980).

8. J. B. Enns, Ph.D. Thesis, Princeton University, 1982.

9. M. B. Roller, J. Coatings Technology, 54, 33, August 1982.

10. W. Jost, Diffusion in Solids, Liquids, Gases. Academic Press, NY (1960).

11. C. H. Shen and G.S. Springer, J. Composite Materials, 10, 2 (1976).

12. J. F. Carpenter, "Moisture Sensitivity of Epoxy Composites and Structural Adhesives", McDonnell Aircraft Co., Report MDC A2640, December 1973.

13. A. Shimazaki , J. Polymer Sci., Part C, 23, 555 (1968).

14. L. E. Nielsen, J. of Macromolecular Sci., C3, 69 (1969).

15. F. W. Billmeyer, Textbook of Polymer Science. Wiley-Interscience, New York (1968), p. 231.

16. R. G. C. Arridge, and J. H. Speake, Polymer 13, 443 (1972).

17. K. Ueberreiter and G. J. Kanig, J. Colloid Science 7, 569 (1953).

TABLE I. Summary of TBA Data.

T_{cure} (°C)	$t_{liquid\text{-}to\text{-}rubber}$ (min)	t_{vit} (min)	T_{sec} (°C)	$T_{sec\infty}$ (°C)	T_g (°C)	$T_{g\infty}$ (°C)
225	8			-35	215	215
210	11	>2400		-41	204	
205	12	130		-40		208
196	15	135		-42	205	205
175	31	144	-41	-30	203	210
156	67	215	-45	-43	181	211
136	151	337	-47	-35	162	206
120	333	569	-58	-38	145	204
96	1285	1498	-74	-39	124	210
89	1490	1996	-79	-36	108	207
79	2357	3083		-39	97	206

TABLE II. Gel Times from Gel Fraction Experiments.

Temperature (°C)	Gel Time (min)	
	Air	Helium
202	9	
185	15	15
180	18	
173	30	
171	38	
168		32
165	48	
156		49
152	73	
151		62
147		77
140	110	
139		120
132		135
120	315	
102	920	

TABLE III. Density, Tg, Diffusivity, Absorptivity and Equilibrium Moisture Content as a Function of Cure.

Cure Time at 175°C (min)	Tg (°C)	Density (g/ml) at 25°C	Absorptivity × 10^2 at 25°C		Relative Humidity (%) 31	51	79.3	93
50	135	1.2370	2.2340	M_∞*	0.474	1.074	1.584	1.908
				D_x†	1.2656	1.6900	1.1587	1.1868
100	160	1.2357	2.4368	M_∞	0.696	1.136	1.803	2.224
				D_x	1.1718	1.7707	1.1984	1.1894
180	185	1.2339	2.9618	M_∞	0.918	1.650	2.429	2.771
				D_x	1.2932	1.5885	1.2291	1.2360
600	195	1.2334	3.1933	M_∞	0.831	1.737	2.426	2.897
				D_x	1.4094	1.7170	1.1705	1.2127

*$M_\infty = \frac{\text{moisture}}{\text{dry weight}} \times 100$ at 25°C

†D_x (cm^2/sec) × 10^{-9} at 25°C

FIGURE CAPTIONS

1. Time-Temperature-Transformation (TTT) Cure Diagram (Schematic).
2. Chemical Structures of Reactants and Crosslinking Site.
3. Isothermal TBA Spectra
   a) Relative Rigidity
   b) Logarithmic Decrement.
4. T_{sec} and Tg Versus Cure Temperature; *as cured, + post-cured.
5. TBA Spectra after Curing at 175°C for various times:
   175 to -190 to 250 to -190°C at 1.5°C/min.
   a) Relative Rigidity
   b) Logarithmic Decrement.
6. Tg Versus Cure Time at 175°C.
7. Torsion Pendulum Spectra of Film: -190 to 250°C (after partial cure at 175°C); 250 to -190°C (after full cure).
8. Gel Fraction Versus Cure Time at Various Temperatures
   a & b) in air, c) in helium.
9. Water Absorption Versus Time$^{\frac{1}{2}}$ at 31% Relative Humidity. Cure time at 175°C: ◇ 50 min., △ 100 min., □ 180 min., ○ 600 min.
10. Water Absorption Versus Time$^{\frac{1}{2}}$ at 51% Relative Humidity (See caption for Figure 9).
11. Water Absorption Versus Time$^{\frac{1}{2}}$ at 79.3% Relative Humidity (See caption for Figure 9).
12. Water Absorption Versus Time$^{\frac{1}{2}}$ at 93% Relative Humidity (See caption for Figure 9).

13. Density Gradient Column Data.

    * Calibrated Floats.

    Specimens cured at 175°C: ◇ 50 min.,△ 100 min.,□ 180 min.,○ 600 min.

14. TTT Cure Diagram. The maximum temperature (Tg_∞) above which vitrification will not occur on isothermal cure is shown as a horizontal dashed line. The temperature of 175°C was selected for preparation of specimens with different extents of cure.

15. Arrhenius Plot of Gel Points and TBA Data.

    △ gel fraction (in air),

    ▽ gel fraction (in helium),

    \+ liquid-to-rubber transformation (TBA),

    ○ vitrification (TBA).

16. Equilibrium Moisture Content Versus Relative Humidity.

    Specimens cured at 175°C for:

    ◇ 50 min,

    △ 100 min,

    □ 180 min,

    ○ 600 min.

17. Absorptivity Versus Specific Volume.

18. Volume-Temperature Plots of a Thermoset with Two Levels of Crosslink Density (Schematic).

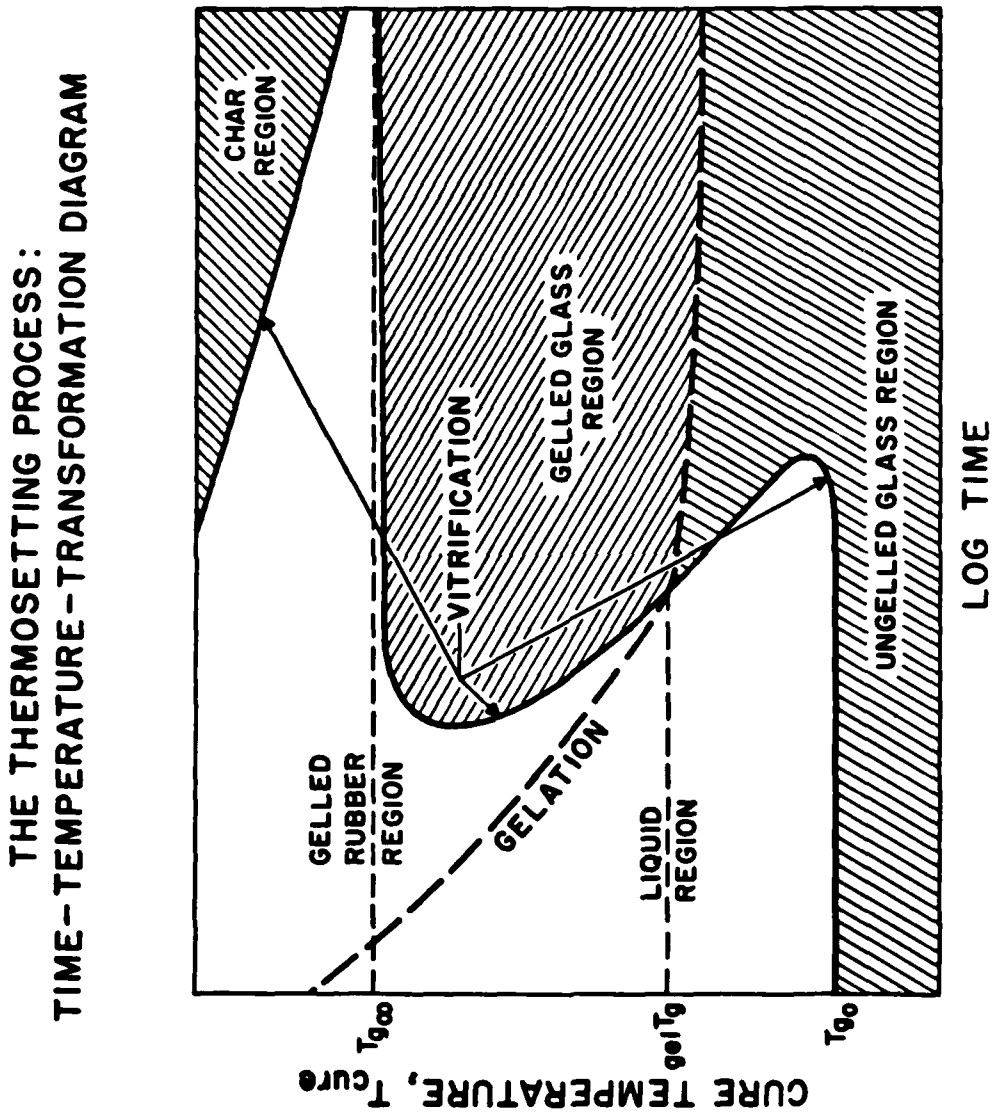
THE THERMOSETTING PROCESS:
TIME-TEMPERATURE-TRANSFORMATION DIAGRAM
CHAR REGION
VITRIFICATION
GELLED GLASS REGION
UNGELLED GLASS REGION
GELLED RUBBER REGION
GELATION
LIQUID REGION
$T_{g\infty}$
T_{gel}
T_{go}
CURE TEMPERATURE, T_{cure}
LOG TIME

Fig. 1

EPOXY: Diglycidyl Ether of Bisphenol A (EPON 828)

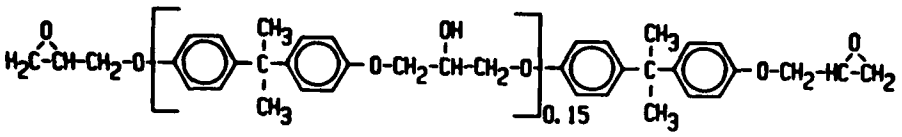

+

AMINE: 4,4'-Diaminodiphenyl Sulfone (DDS)

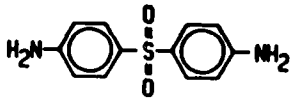

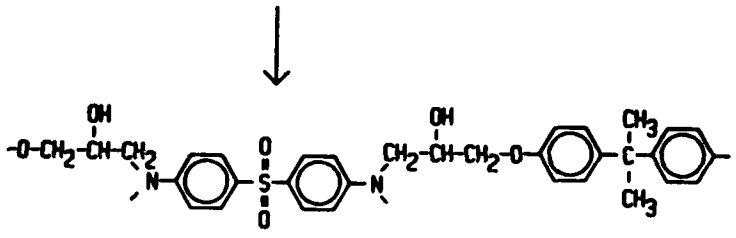

CROSSLINKED NETWORK

Fig. 2

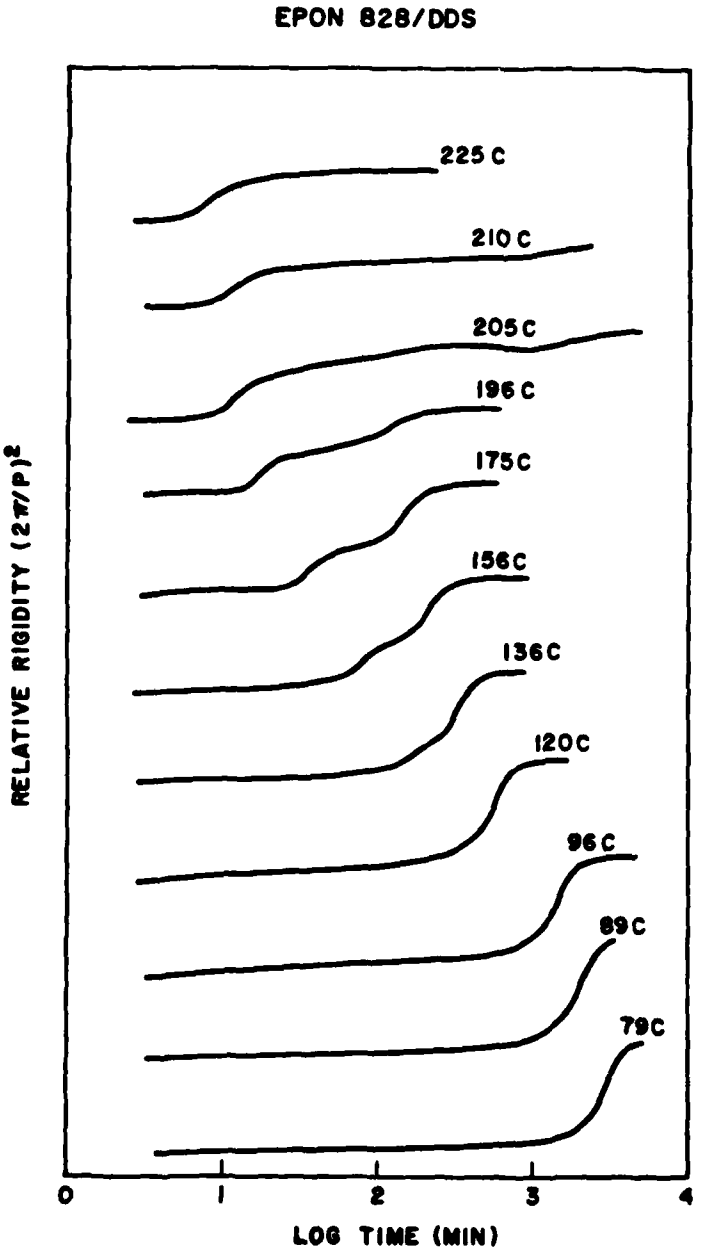
EPON 828/DDS
225 C
210 C
205 C
196 C
175 C
156 C
136 C
120 C
96 C
89 C
79 C
RELATIVE RIGIDITY $(2\pi/P)^2$
0
1
2
3
4
LOG TIME (MIN)

Fig. 3a

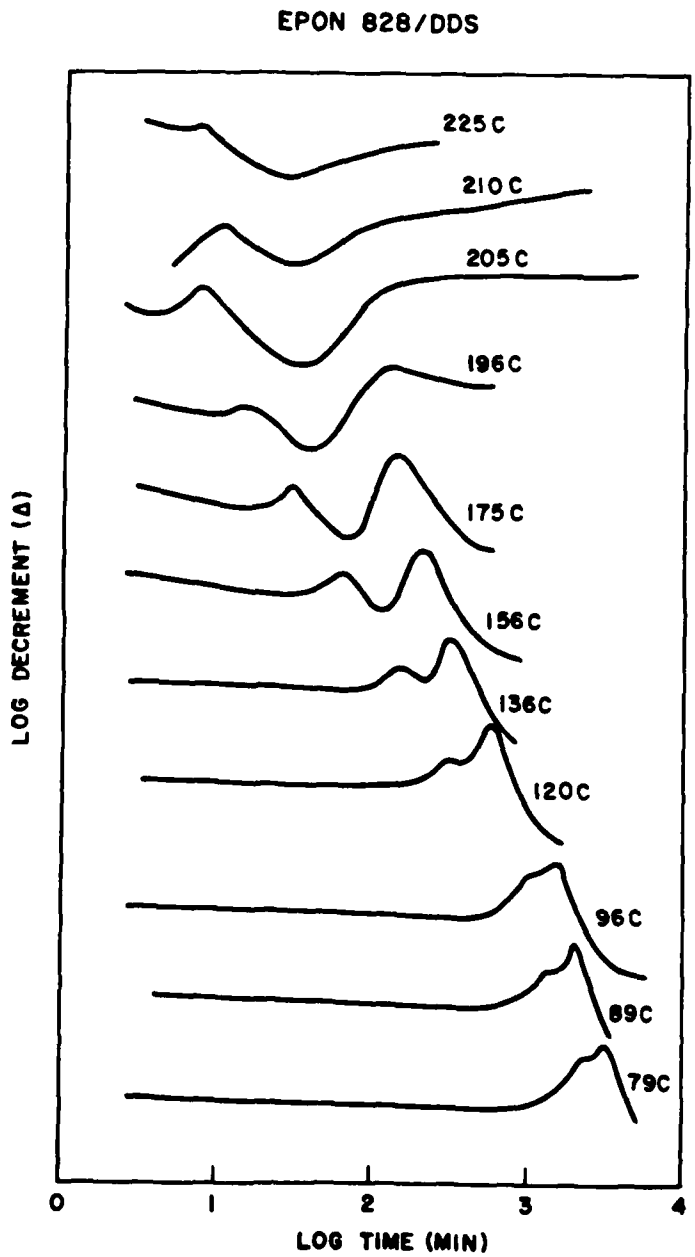
EPON 828/DDS
225C
210C
205C
196C
175C
156C
136C
120C
96C
89C
79C
LOG DECREMENT (Δ)
0
1
2
3
4
LOG TIME (MIN)

Fig. 3b

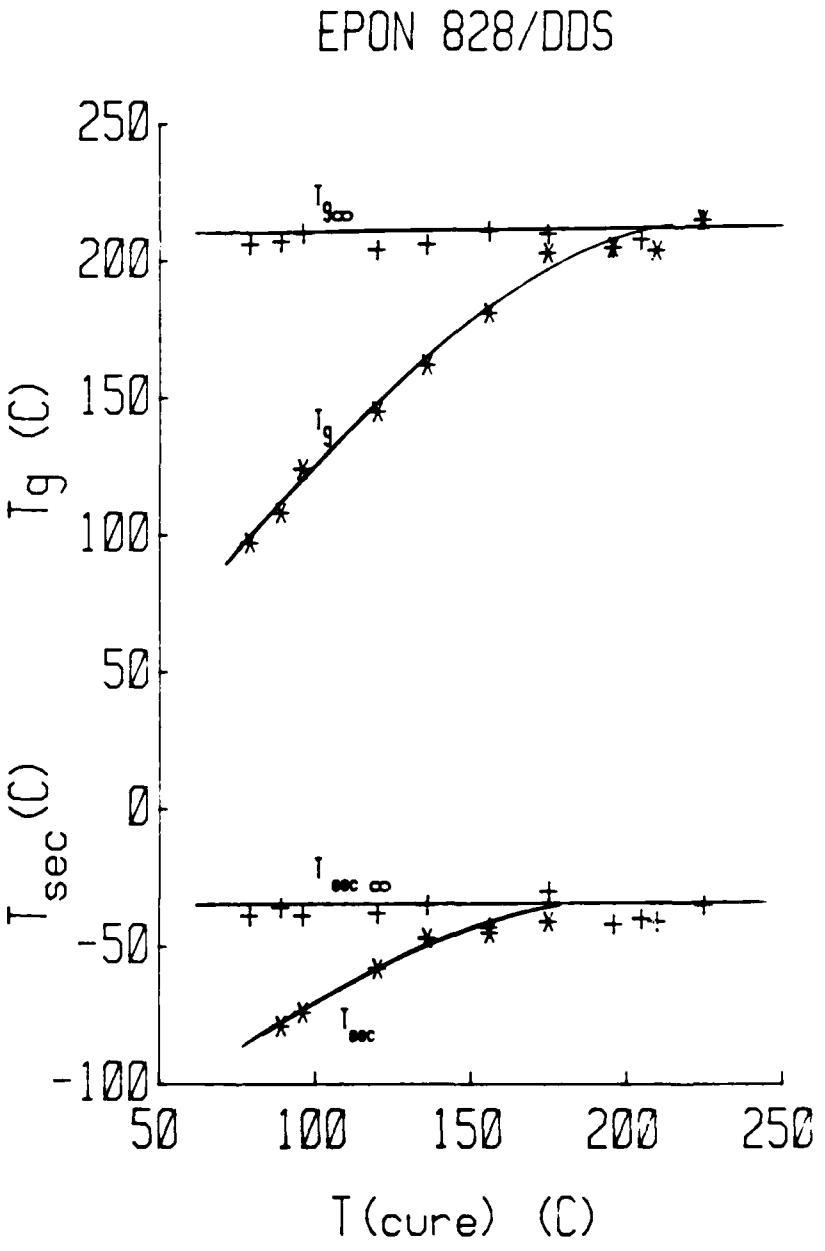
EPON 828/DDS
250
200
150
100
50
0
-50
-100
Tg (C)
Tsec (C)
Tg∞
Tg
Tsec ∞
Tsec
50
100
150
200
250
T(cure) (C)

Fig. 4

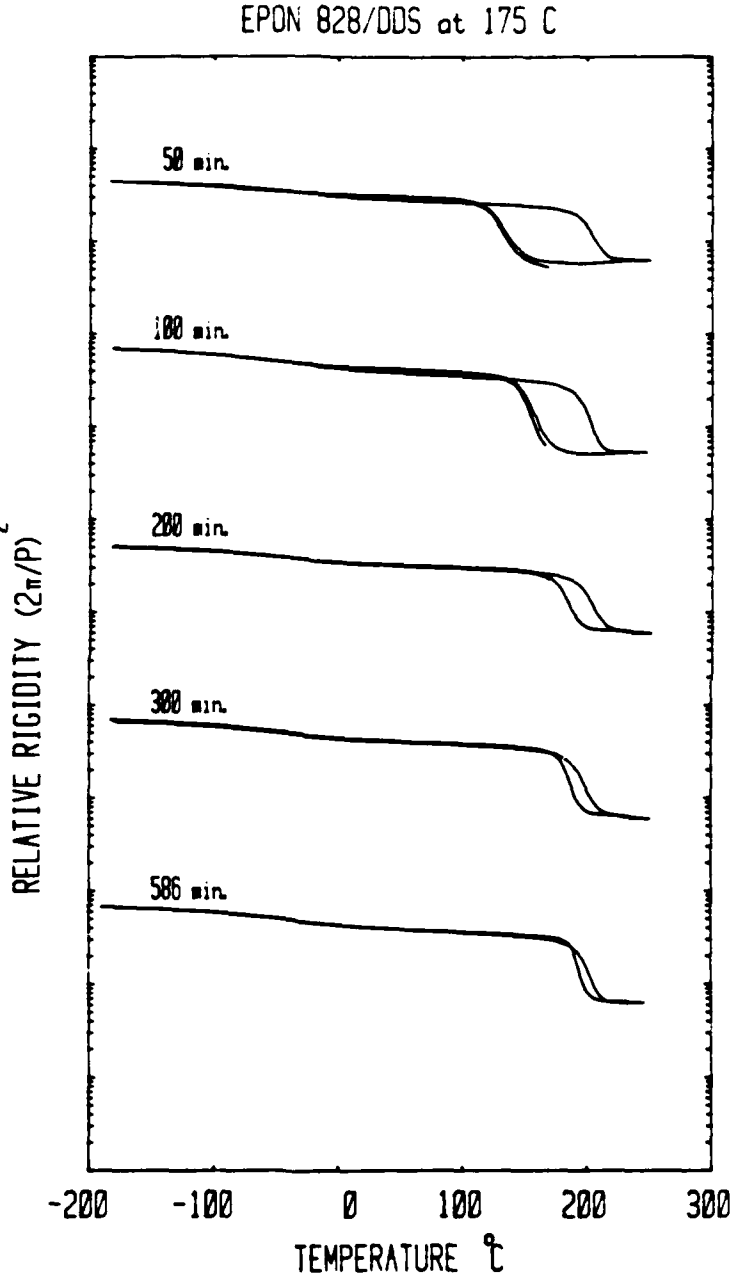
EPON 828/DDS at 175 C
50 min.
100 min.
200 min.
300 min.
586 min.
RELATIVE RIGIDITY (2π/P)²
-200
-100
0
100
200
300
TEMPERATURE °C

Fig. 5a

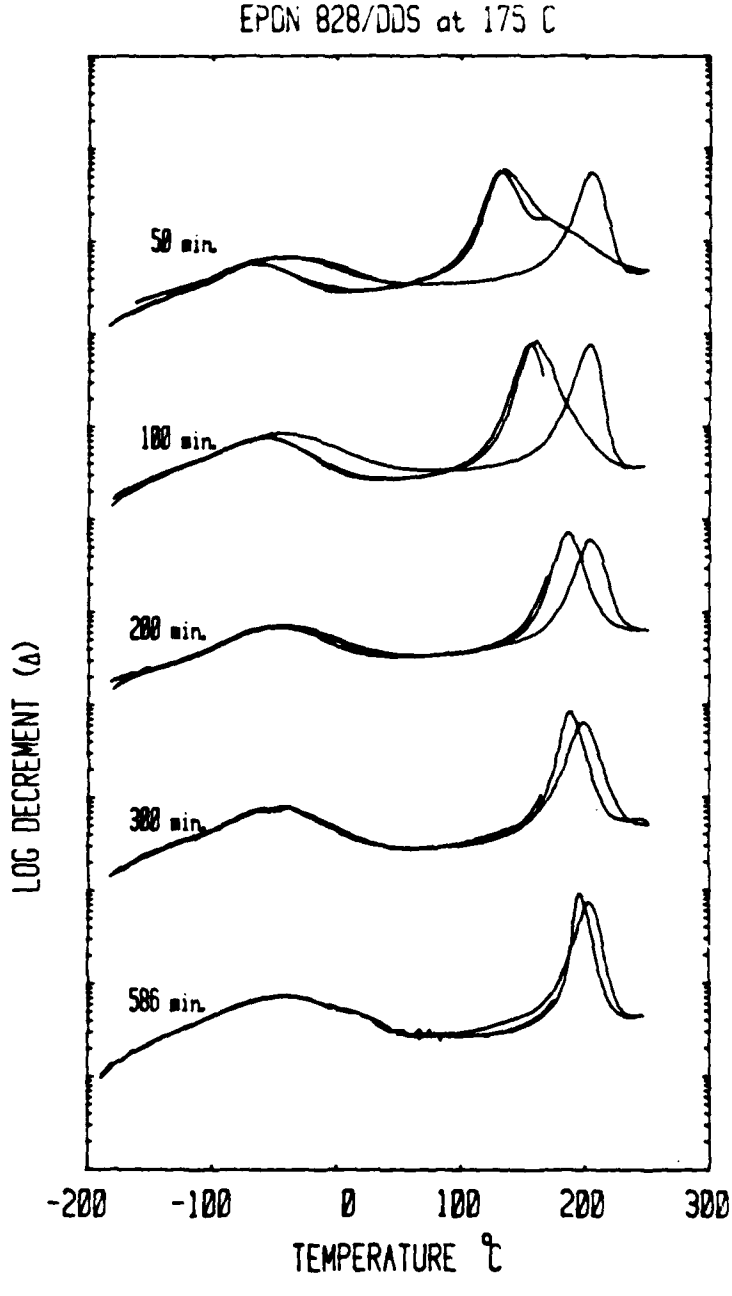
EPON 828/DDS at 175 C
50 min.
100 min.
200 min.
300 min.
586 min.
LOG DECREMENT (Δ)
-200
-100
0
100
200
300
TEMPERATURE °C

Fig. 5b

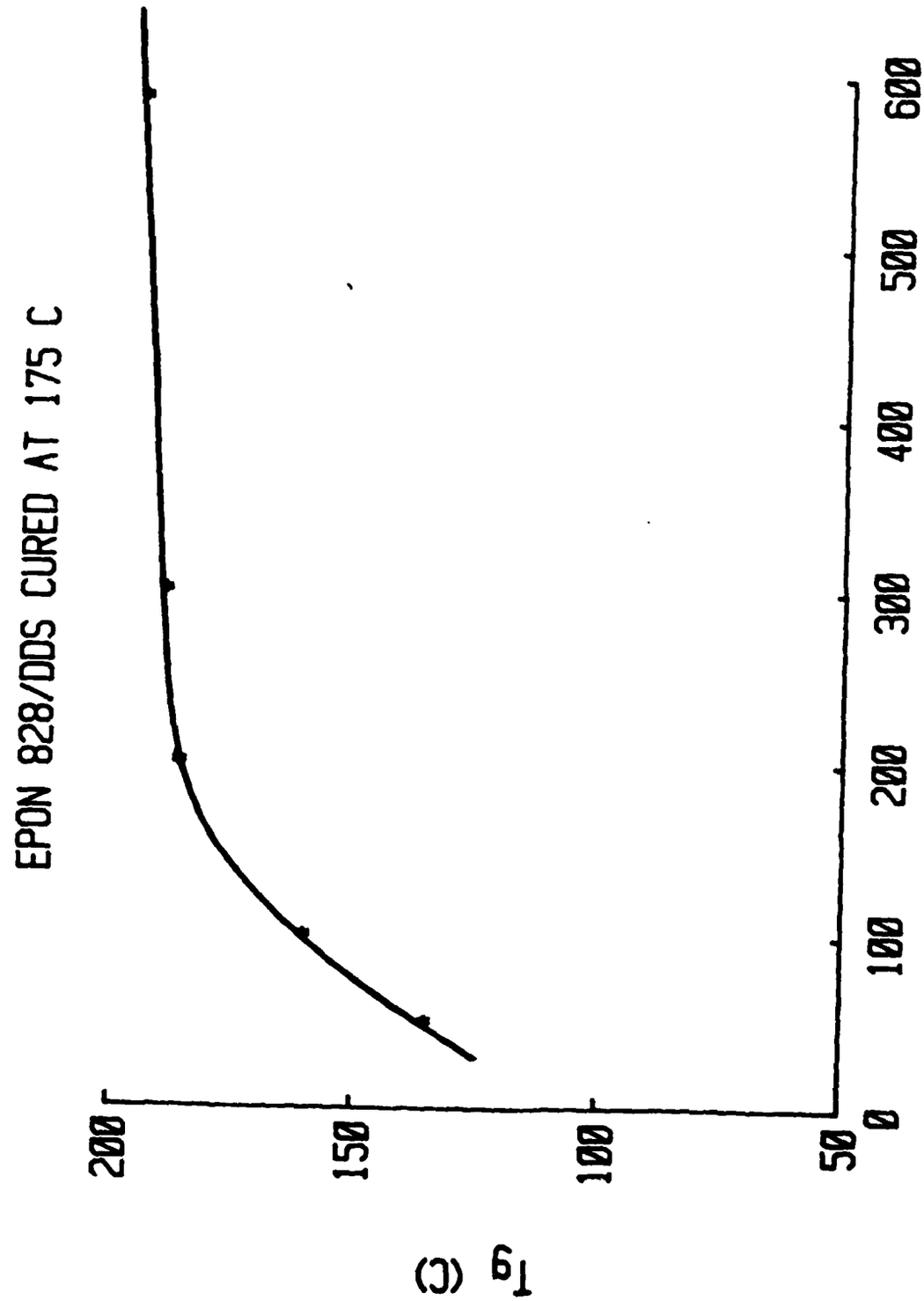
EPON 828/DDS CURED AT 175 C
T_g (C)
200
150
100
50
0
100
200
300
400
500
600
CURE TIME (min)

Fig. 6

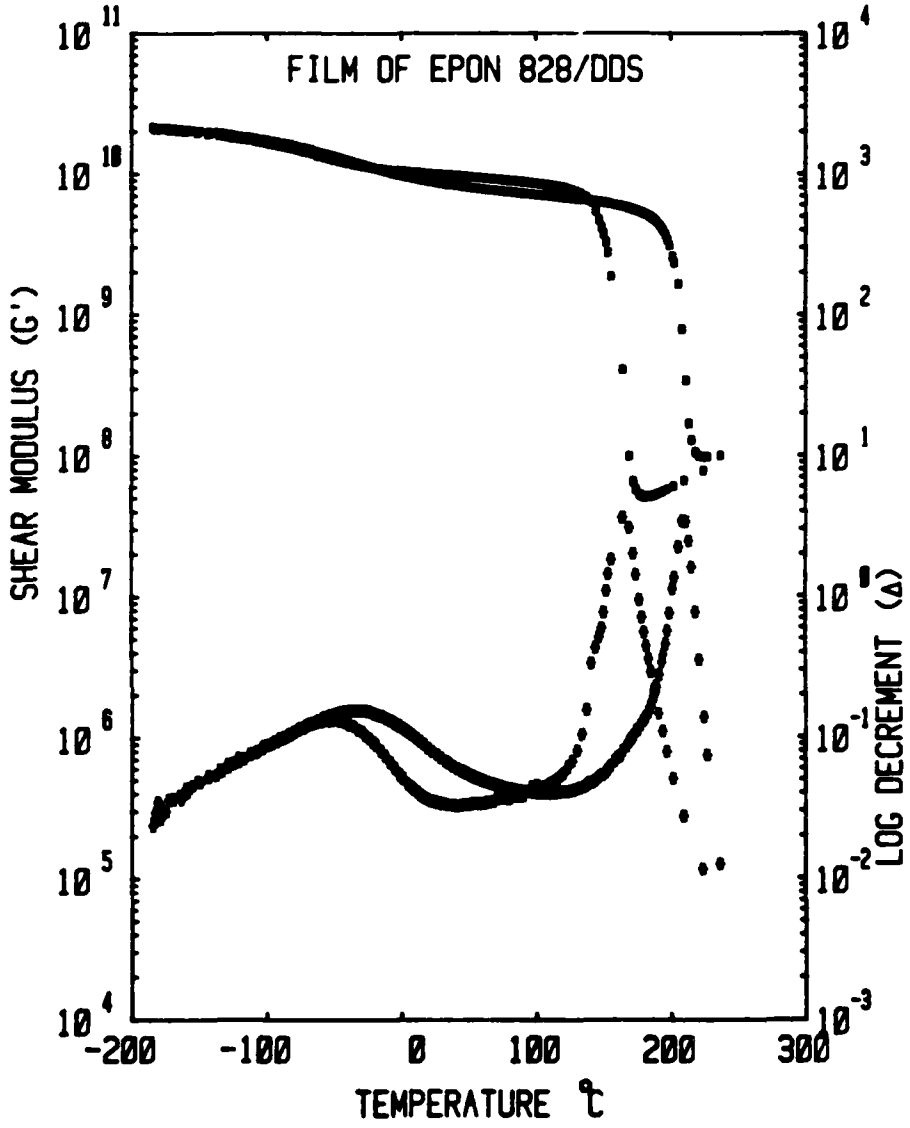
FILM OF EPON 828/DDS
SHEAR MODULUS (G')
LOG DECREMENT (Δ)
TEMPERATURE °C
10^11
10^10
10^9
10^8
10^7
10^6
10^5
10^4
10^4
10^3
10^2
10^1
10^0
10^-1
10^-2
10^-3
-200
-100
0
100
200
300

Fig. 7

GEL FRACTION EPON 828/DDS
102 C
120 C
140 C
152 C
1.0
0.8
0.6
0.4
0.2
0.0
GEL FRACTION
0
200
400
600
800
1000
1200
TIME (min)

Fig. 8a

GEL FRACTION EPON 828/DDS
202 C
185 C
180 C
171 C
GEL FRACTION
1.0
0.8
0.6
0.4
0.2
0.00
10
20
30
40
50
60
TIME (min)

Fig. 8b

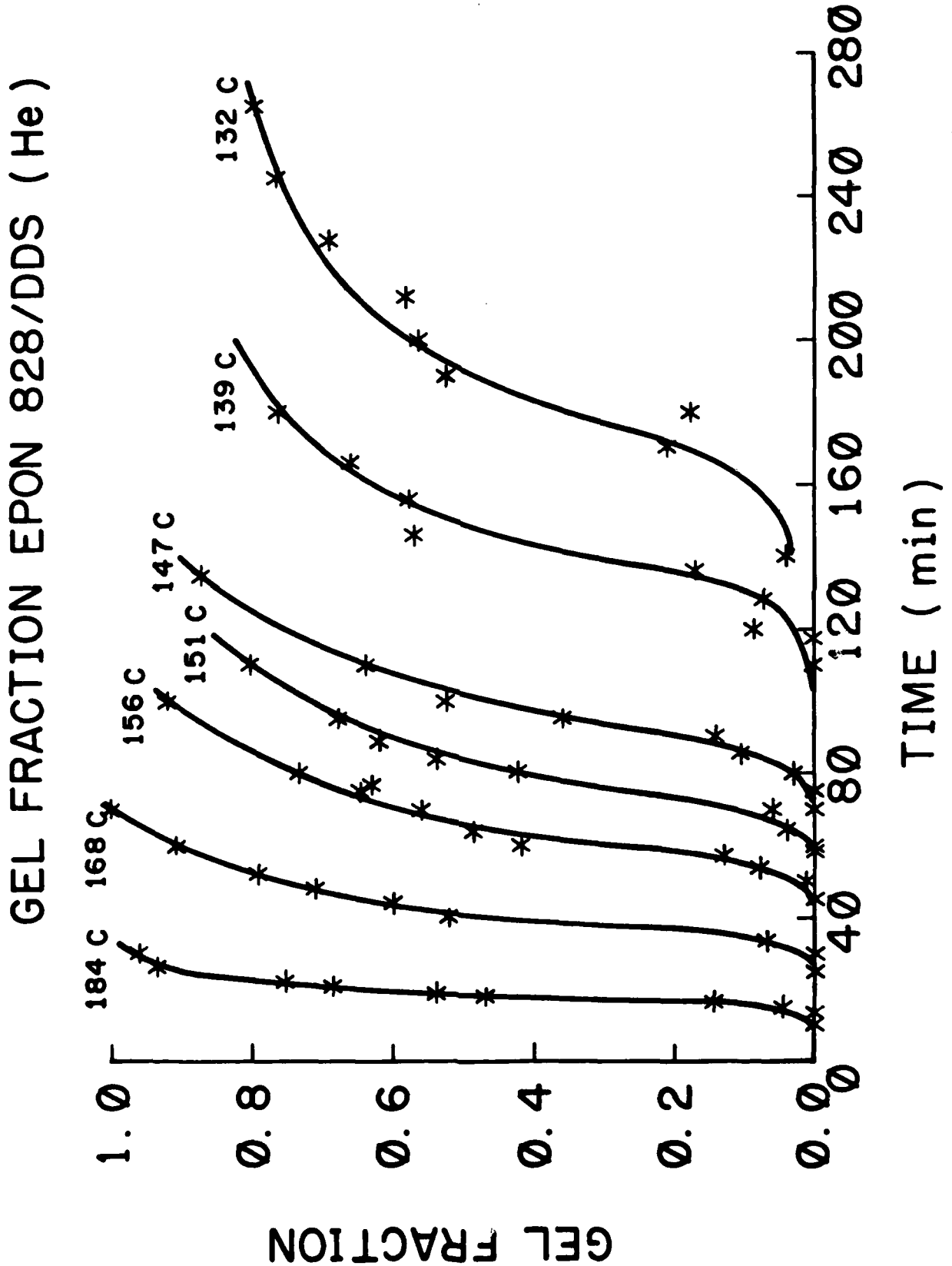
GEL FRACTION EPON 828/DDS (He)
GEL FRACTION
TIME (min)
1.0
0.8
0.6
0.4
0.2
0.0
0
40
80
120
160
200
240
280
132 C
139 C
147 C
151 C
156 C
168 C
184 C

Fig. 8c

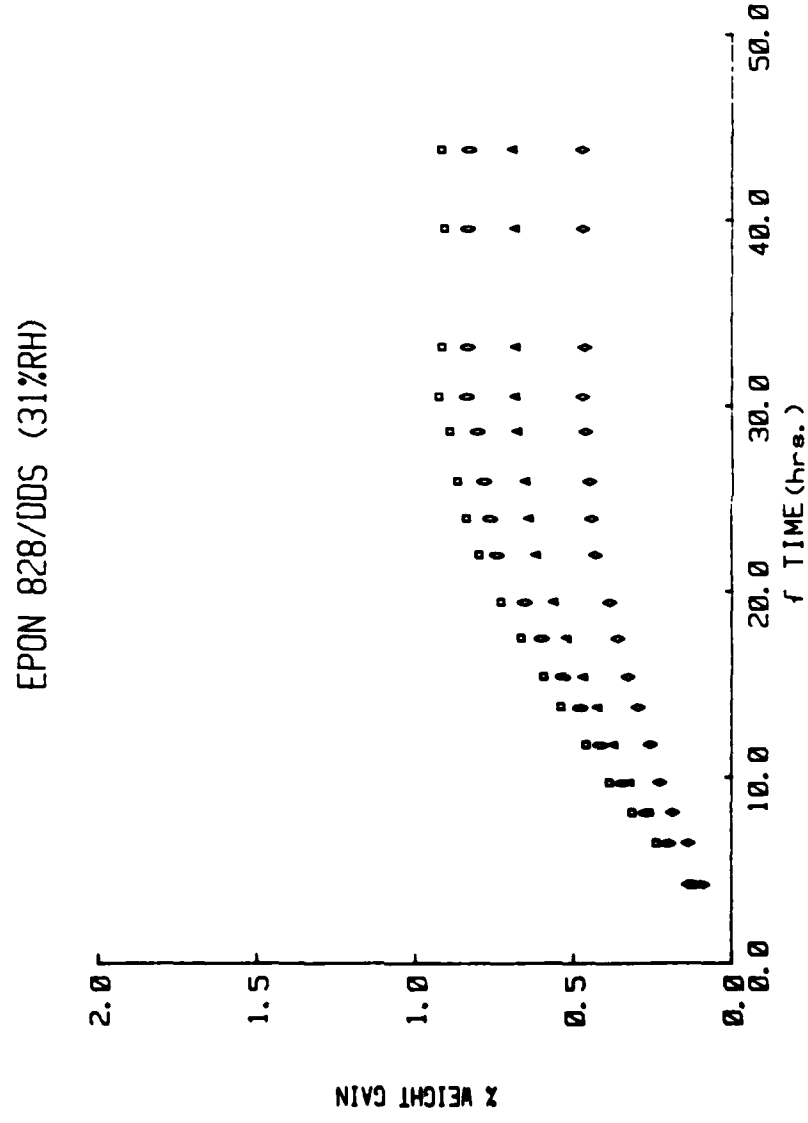
EPON 828/DDS (31%RH)
% WEIGHT GAIN
2.0
1.5
1.0
0.5
0.0
0.0
10.0
20.0
30.0
40.0
50.0
√ TIME (hrs.)

Fig. 9

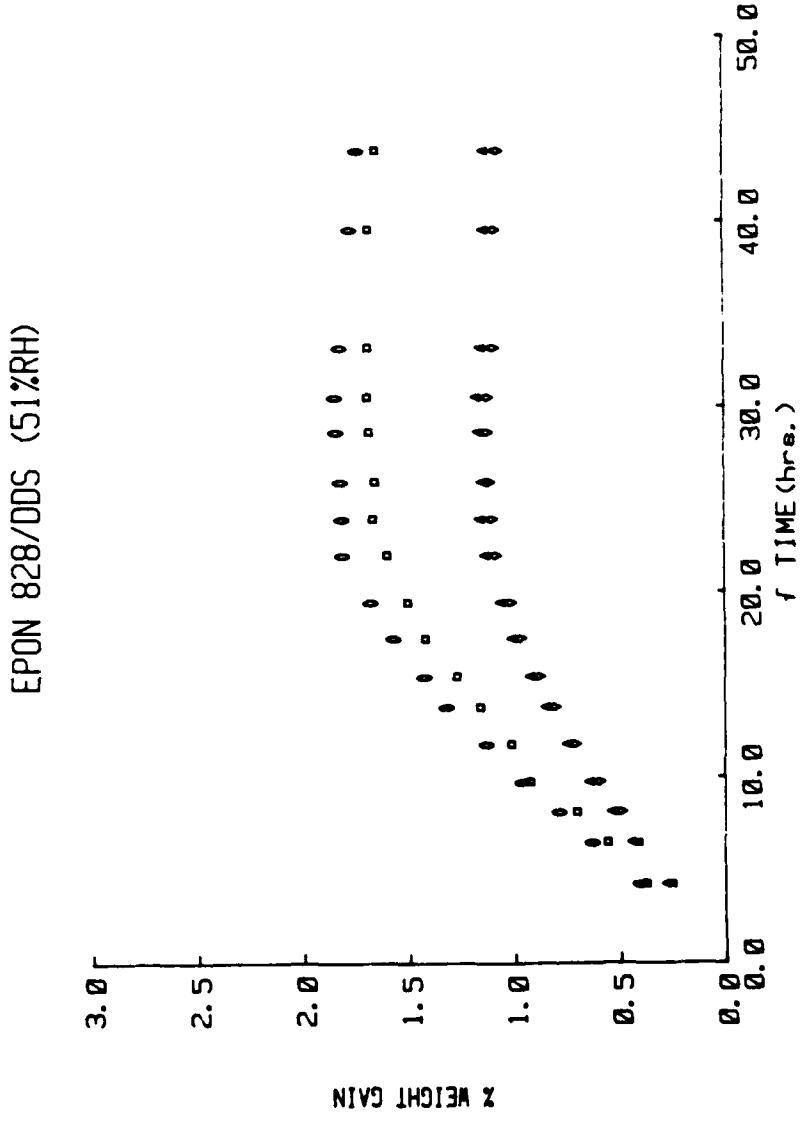
EPON 828/DDS (51%RH)
% WEIGHT GAIN
3.0
2.5
2.0
1.5
1.0
0.5
0.0
0.0
10.0
20.0
30.0
40.0
50.0
t TIME (hrs.)

Fig. 10

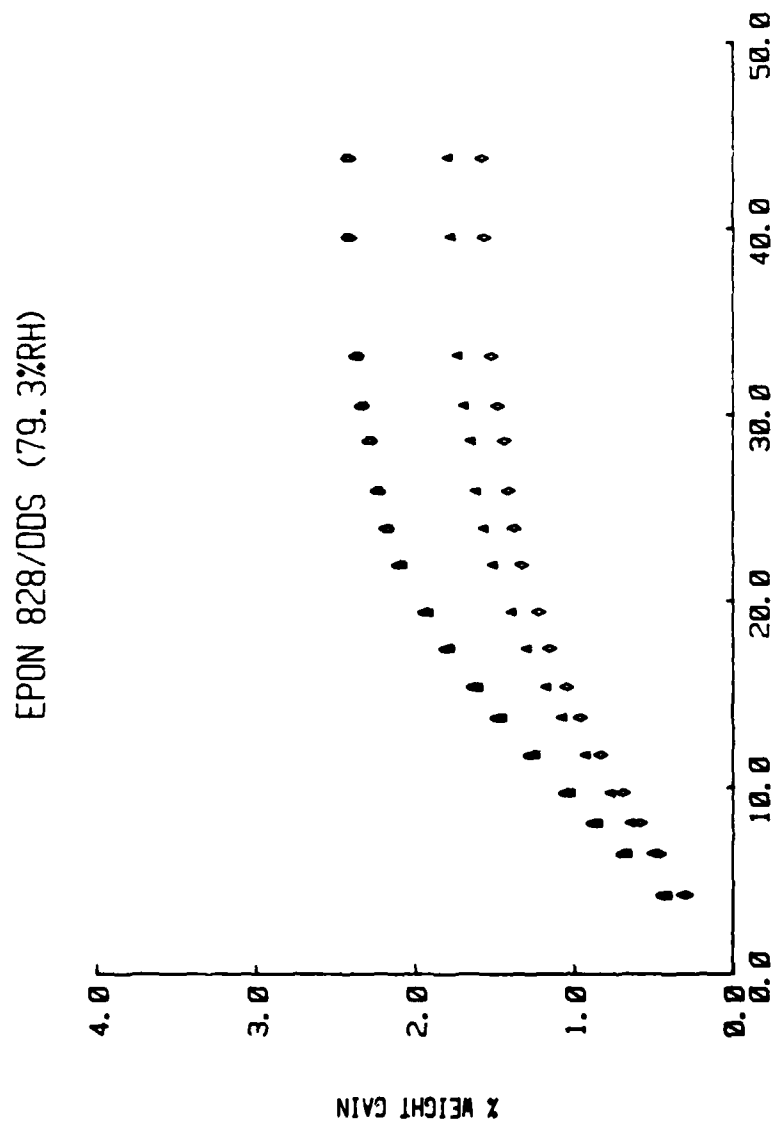
EPON 828/DDS (79.3%RH)
% WEIGHT GAIN
4.0
3.0
2.0
1.0
0.0
0.0
10.0
20.0
30.0
40.0
50.0
√ TIME (hrs.)

Fig. 11

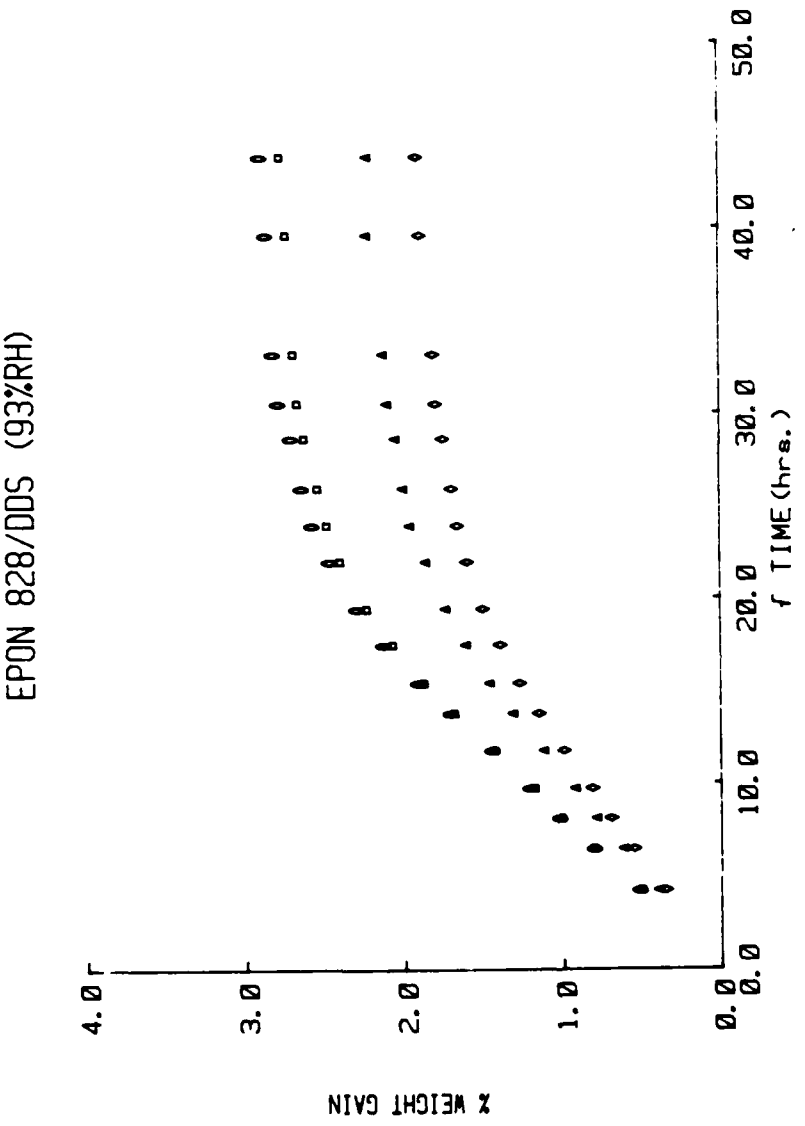
EPON 828/DDS (93%RH)
% WEIGHT GAIN
4.0
3.0
2.0
1.0
0.0
0.0
10.0
20.0
30.0
40.0
50.0
√ TIME (hrs.)

Fig. 12

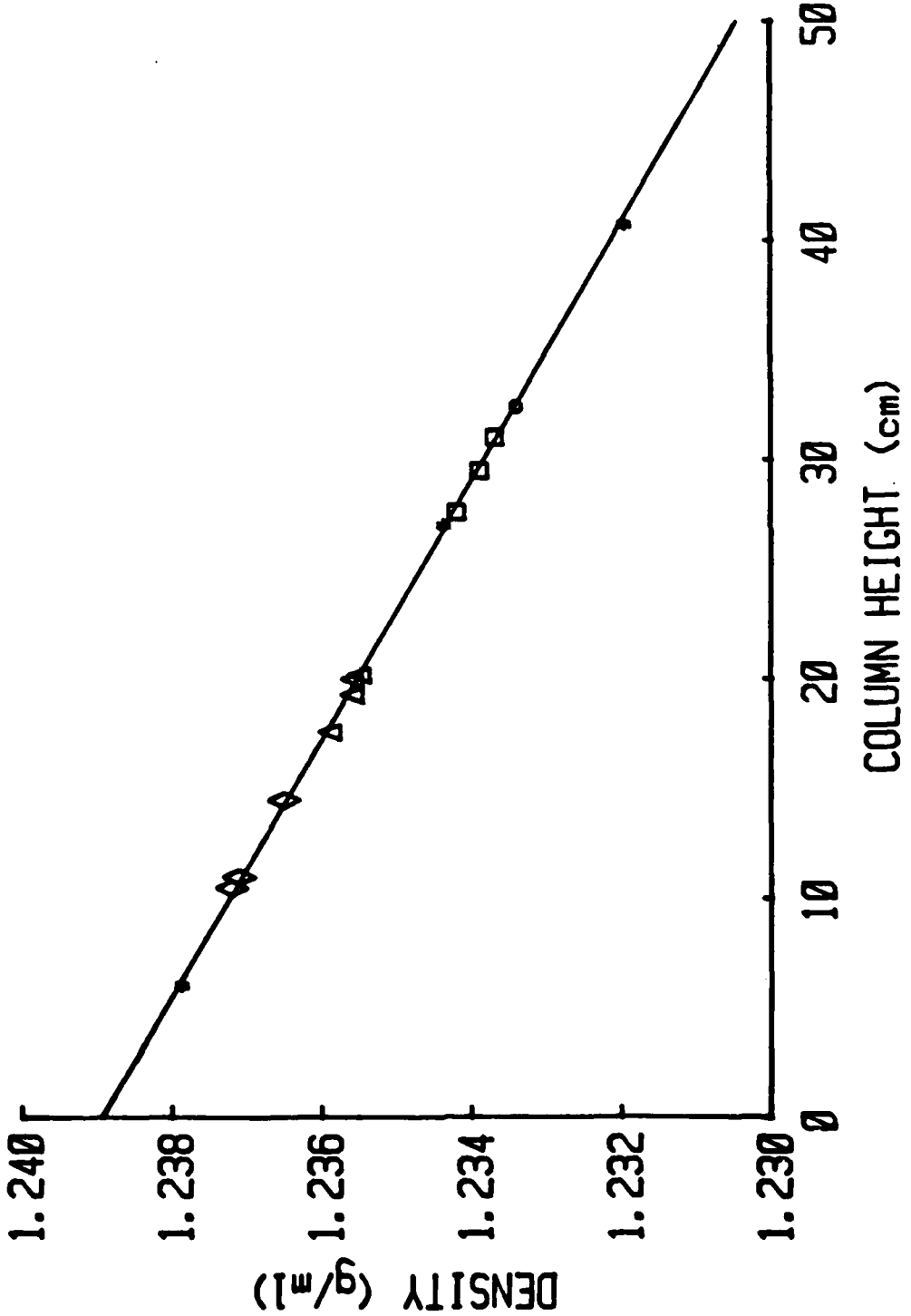
DENSITY GRADIENT COLUMN CALIBRATION CURVE
DENSITY (g/ml)
1.240
1.238
1.236
1.234
1.232
1.230
0
10
20
30
40
50
COLUMN HEIGHT (cm)

Fig. 13

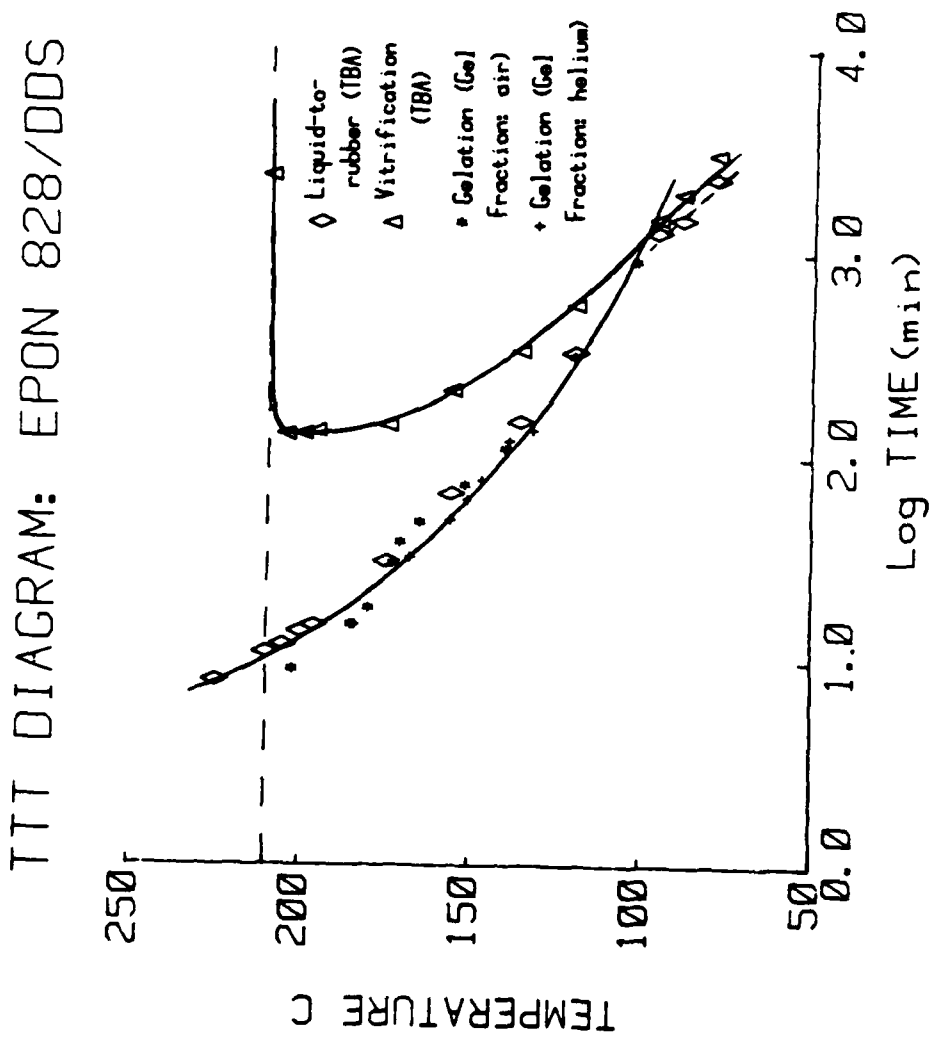
TTT DIAGRAM: EPON 828/DDS
◊ Liquid-to-rubber (TBA)
Δ Vitrification (TBA)
• Gelation (Gel Fraction: air)
+ Gelation (Gel Fraction: helium)
TEMPERATURE C
250
200
150
100
50
0.0
1.0
2.0
3.0
4.0
Log TIME(min)

Fig. 14

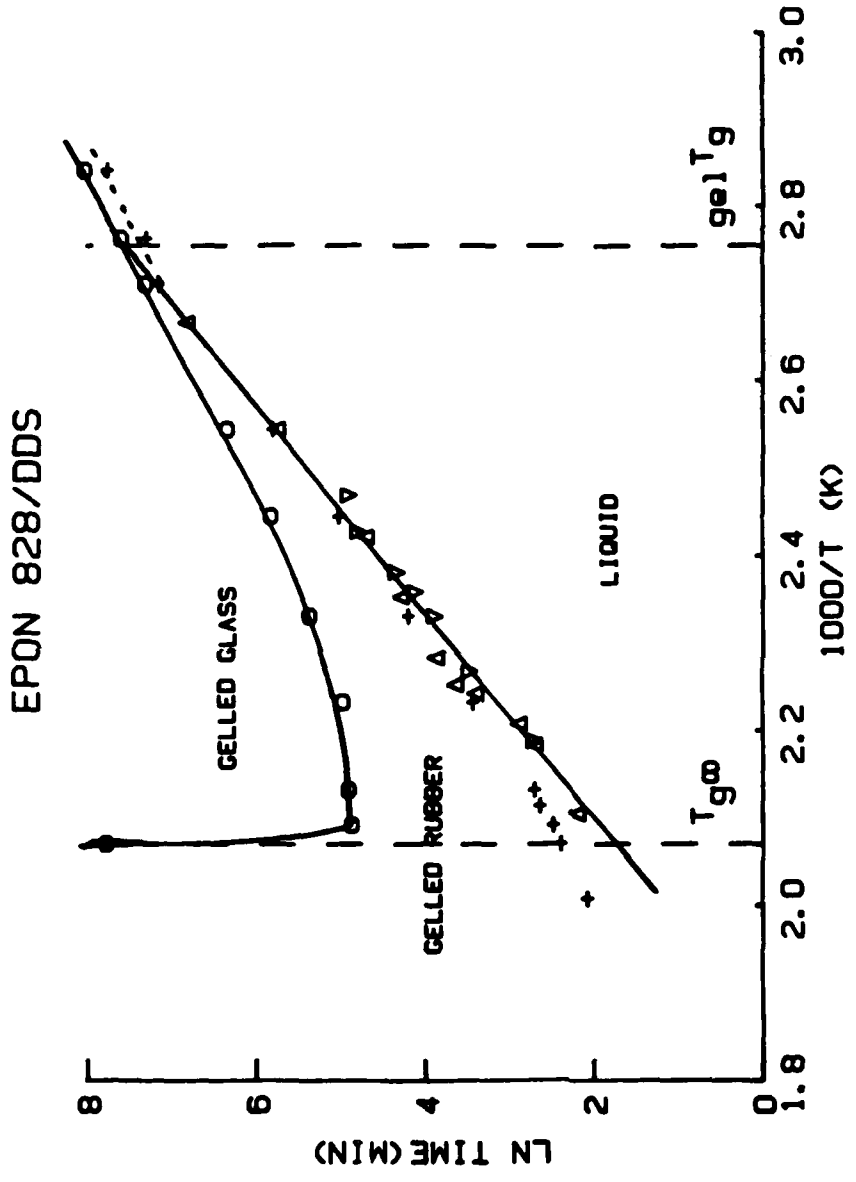
EPON 828/DDS
GELLED GLASS
GELLED RUBBER
LIQUID
T_{gel}
$T_{g\infty}$
LN TIME (MIN)
1000/T (K)
8
6
4
2
0
1.8
2.0
2.2
2.4
2.6
2.8
3.0

Fig. 15

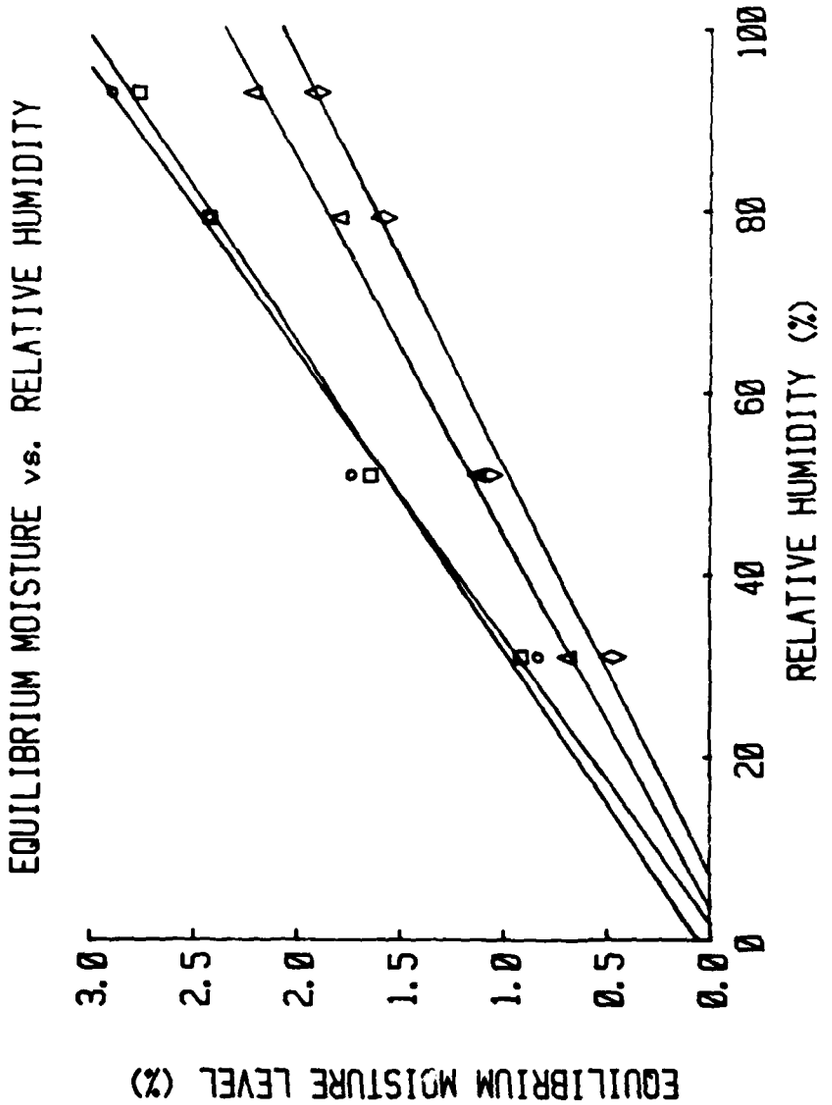
EQUILIBRIUM MOISTURE vs. RELATIVE HUMIDITY
EQUILIBRIUM MOISTURE LEVEL (%)
RELATIVE HUMIDITY (%)
3.0
2.5
2.0
1.5
1.0
0.5
0.0
0
20
40
60
80
100

Fig. 16

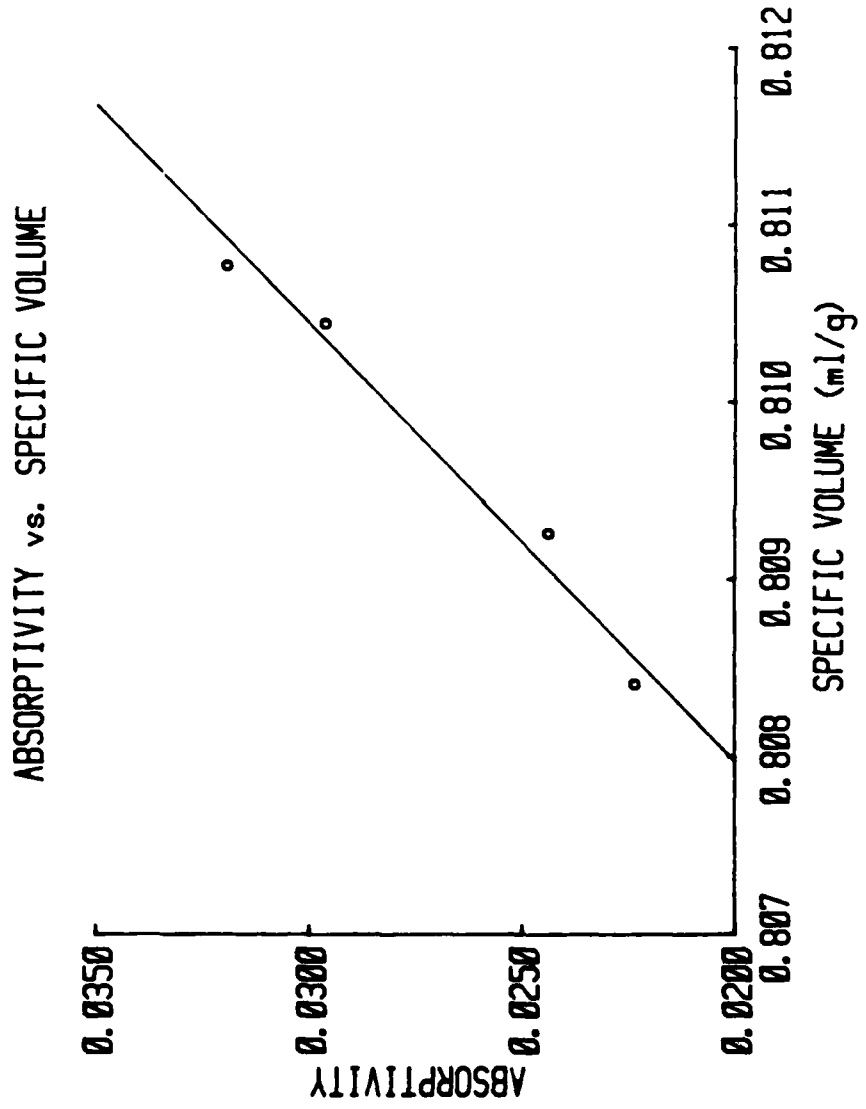
ABSORPTIVITY vs. SPECIFIC VOLUME
ABSORPTIVITY
0.0350
0.0300
0.0250
0.0200
0.807
0.808
0.809
0.810
0.811
0.812
SPECIFIC VOLUME (ml/g)

Fig. 17

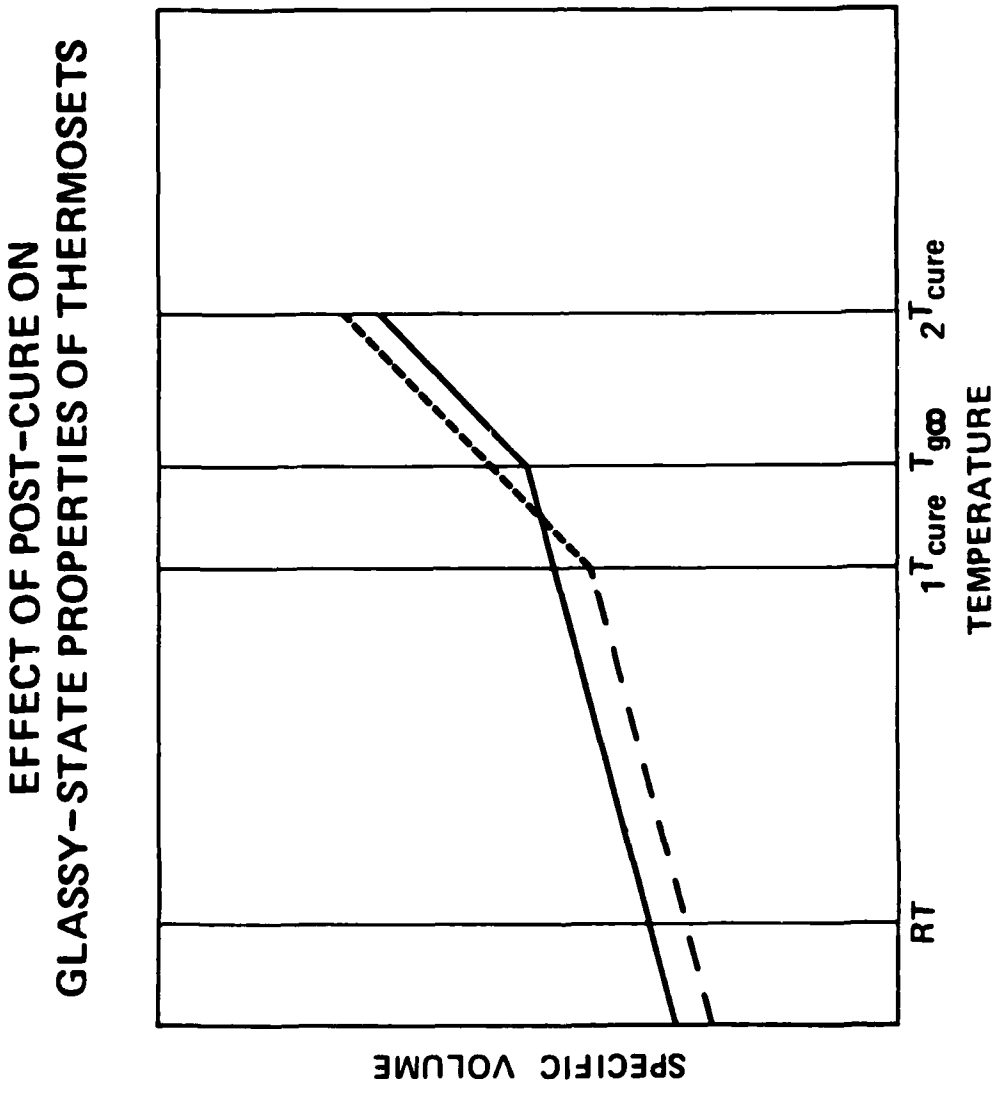
EFFECT OF POST-CURE ON
GLASSY-STATE PROPERTIES OF THERMOSETS
SPECIFIC VOLUME
TEMPERATURE
RT
$1T_{cure}$
$T_{g\infty}$
$2T_{cure}$

Fig. 18

472:GAN:716-4
94/GEN

TECHNICAL REPORT DISTRIBUTION LIST, GEN

	No. Copies
Office of Naval Research Attn: Code 413 800 North Quincy Street Arlington, Virginia 22217	2
ONR Pasadena Detachment Attn: Dr. R. J. Marcus 1030 East Green Street Pasadena, California 91106	1
Commander, Naval Air Systems Command Attn: Code 310C (H. Rosenwasser) Department of the Navy Washington, D.C. 20360	1
Defense Technical Information Center Building 5, Cameron Station Alexandria, Virginia 22314	12
Dr. Fred Saalfeld Chemistry Division, Code 6100 Naval Research Laboratory Washington, D.C. 20375	1
U.S. Army Research Office Attn: CRD-AA-IP P. O. Box 12211 Research Triangle Park, N.C. 27709	1
Mr. Vincent Schaper DTNSRDC Code 2803 Annapolis, Maryland 21402	1
Naval Ocean Systems Center Attn: Dr. S. Yamamoto Marine Sciences Division San Diego, California 91232	1
Naval Ocean Systems Center Attn: Mr. Joe McCartney San Diego, California 92152	1
Naval Weapons Center Attn: Dr. A. B. Amster, Chemistry Division China Lake, California 93555	1
Naval Civil Engineering Laboratory Attn: Dr. R. W. Drisko Port Hueneme, California 93401	1
Dean William Tolles Naval Postgraduate School Monterey, California 93940	1
Scientific Advisor Commandant of the Marine Corps (Code RD-1) Washington, D.C. 20380	1
Naval Ship Research and Development Center Attn: Dr. G. Bosmajian, Applied Chemistry Division Annapolis, Maryland 21401	1
Mr. John Boyle Materials Branch Naval Ship Engineering Center Philadelphia, Pennsylvania 19112	1
Mr. A. M. Anzalone Administrative Librarian PLASTEC/ARRADCOM Bldg 3401 Dover, New Jersey 07801	1

472:GAN:716-4
94/356A-B

TECHNICAL REPORT DISTRIBUTION LIST, 356A

	No. Copies
Dr. M. Broadhurst Bulk Properties Section National Bureau of Standards U. S. Department of Commerce Washington, D.C. 20234	2
Naval Surface Weapons Center Attn: Dr. J. M. Augl, Dr. B. Hartman White Oak Silver Spring, Maryland 20910	1
Dr. G. Goodman Globe Union Incorporated 5757 North Green Bay Avenue Milwaukee, Wisconsin 53201	1
Professor Hatsuo Ishida Department of Macromolecular Science Case-Western Reserve University Cleveland, Ohio 44106	1
Dr. David Soong Department of Chemical Engineering University of California Berkeley, California 94720	1
Dr. Curtis W. Frank Department of Chemical Engineering Stanford University Stanford, California 94035	1
Picatinny Arsenal Attn: A. M. Anzalone, Building 3401 SMUPA-FR-M-D Dover, New Jersey 07801	1
Dr. J. K. Gillham Department of Chemistry Princeton University Princeton, New Jersey 08540	1
Dr. E. Baer Department of Macromolecular Science Case Western Reserve University Cleveland, Ohio 44106	1
Dr. K. D. Pae Department of Mechanics and Materials Science Rutgers University New Brunswick, New Jersey 08903	1
NASA-Lewis Research Center Attn: Dr. T. T. Serofini, MS-49-1 2100 Brookpark Road Cleveland, Ohio 44135	1
Dr. Charles H. Sherman Code TD 121 Naval Underwater Systems Center New London, Connecticut 06320	1
Dr. William Risen Department of Chemistry Brown University Providence, Rhode Island 02191	1
Mr. Robert W. Jones Advanced Projects Manager Hughes Aircraft Company Mail Station D 132 Culver City, California 90230	1
Dr. C. Giori IIT Research Institute 10 West 35 Street Chicago, Illinois 60616	1
Dr. R. S. Roe Department of Materials Science and Metallurgical Engineering University of Cincinnatti Cincinnati, Ohio 45221	1
Dr. Robert E. Cohen Chemical Engineering Department Massachusetts Institute of Technology Cambridge, Massachusetts 02139	1
Dr. T. P. Conlon, Jr., Code 3622 Sandia Laboratories Sandia Corporation Albuquerque, New Mexico	1

472:GAN:716-4
94/356A-B

TECHNICAL REPORT DISTRIBUTION LIST, 356A

	No. Copies
Dr. Martin Kaufman Code 38506 Naval Weapons Center China Lake, California 93555	1
Professor S. Senturia Department of Electrical Engineering Massachusetts Institute of Technology Cambridge, Massachusetts 02139	1
Dr. T. J. Reinhart, Jr., Chief Composite and Fibrous Materials Branch Nonmetallic Materials Division Department of the Air Force Air Force Materials Laboratory (AFSC) Wright-Patterson AFB, Ohio 45433	1
Dr. J. Lando Department of Macromolecular Science Case Western Reserve University Cleveland, Ohio 44106	1
Dr. J. White Chemical and Metallurgical Engineering University of Tennessee Knoxville, Tennessee 37916	1
Dr. J. A. Manson Materials Research Center Lehigh University Bethlehem, Pennsylvania 18015	1
Dr. R. F. Helmreich Contract RD&E Dow Chemical Co. Midland, Michigan 48640	1
Dr. R. S. Porter Department of Polymer Science and Engineering University of Massachusetts Amherst, Massachusetts 01002	1
Professor Garth Wilkes Department of Chemical Engineering Virginia Polytechnic Institute and State University Blacksburg, Virginia 24061	1
Professor C. S. Paik Sung Department of Materials Sciences and Engineering Room 8-109 Massachusetts Institute of Technology Cambridge, Massachusetts 02139	1
Professor Brian Newman Department of Mechanics and Materials Science Rutgers, The State University Piscataway, New Jersey 08854	1
Dr. John Lundberg School of Textile Engineering Georgia Institute of Technology Atlanta, Georgia 30332	1